Real-Time Implementation of a Three-Phase THSeAF Based on a VSC and a P+R Controller to Improve the Power Quality of Weak Distribution Systems

Alireza Javadi, *Member, IEEE*, Lyne Woodward, *Member, IEEE*, and Kamal Al-Haddad, *Fellow, IEEE*

***Abstract*—This paper proposes a novel three-phase transformerless hybrid series active filter (THSeAF) based on voltage-fed type of converters (VSCs) to address major power quality issues related to residential and commercial buildings. This power quality compensator presents an affordable solution to overcome current-related issues as well as integrating renewables to ensure a sustainable supply to the loads. The controller is based on a novel combination of the synchronous reference frame and *pq* theory to extract voltage and current harmonics as well as voltage unbalances. A proportional resonant (P+R) regulator is producing gate switching signals for the three-phase THSeAF. The generated duty-cycle waveforms will produce compensating voltage to rectify harmonic currents initiated from typical nonlinear loads. The device ensures a reliable and dynamically restored power supply on the load's point of common coupling by means of three auxiliary dc supplies. This paper describes mitigation of power-quality-related issues of a microgrid systems and smart distribution grids along with the proposed solution to enhance the power system performances. A combination of simulations and experimental laboratory results are carried out to validate the study.**

***Index Terms*—Current harmonics, instantaneous power theory, power quality, proportional resonant controller, series hybrid active filter, voltage restoration.**

I. Introduction

THE forecast of a smart grid associated with the continuous increase of switch-mode power converters, drives, as well as domestic and industrial nonlinear loads has created a serious concern on the power quality of the future distribution power systems, as shown in Fig. 1 [1]. Along with integration of renewables into the smart microgrids, expansion of electronic polluting devices as well as electric vehicle charging stations would have harmful impacts on the power quality. Electric vehicle market shows a considerable growth [2]–[4]; therefore, it became crucial to monitor and evaluate their behavior and associated current waveforms when charging [5], [6]. Moreover, in some existing North American EV charging stations, the cars are connected between two phases of the three-phase four-wire system [7], [8], creating heavy unbalances. On the other hand, pushed by social efforts, governments start to investigate more on implementation of renewable energy sources, creating research and developments in this field [9]–[11].

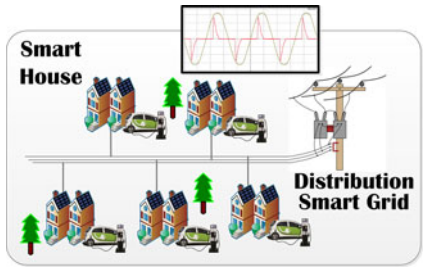

Fig. 1. Smart residential consumer with non-linear electronic loads.

This work proposes an efficient three-phase transformerless hybrid series active filter (THSeAF) capable to rectify current-related issues in the smart microgrids, which also provides sustainable and reliable voltage supply at the point of common coupling (PCC) where residential and commercial buildings are connected with nonlinear time-varying load-side demand [12], [13]. The use of this device will facilitate the integration of energy storage systems and renewables for modern systems [14]. The compensator is connected at the distribution level of the power system to prevent harmonic currents of a load to flow into the grid, while protecting the downstream loads from voltage perturbations coming from the utility and protecting the later from sags and swells [15], [16].

This proposed low-cost configuration ride of the common bulky series transformer is an economic key toward power quality improvement of smart grid's power quality development [17], [18]. This compensator cleans the current harmonics from the utility, and similarly to a dynamic voltage restorer (DVR), the PCC and utility's smart meters will be protected from voltage

Manuscript received December 15, 2016; revised March 4, 2017; accepted April 15, 2017. Date of publication April 25, 2017; date of current version December 1, 2017. This work was supported by NSERC-CRSNG, the Canada Research Chair in Electrical Energy Conversion and Power Electronics, École de Technologie Supérieure of Montreal. Recommended for publication by Associate Editor B. Singh. *(Corresponding author: Alireza Javadi.)*

A. Javadi and L. Woodward are with the Department of Electrical Engineering, École de Technologie Supérieure, University of Quebec, Montreal, QC H3C1K3 Canada (e-mail: alireza.javadi.1@ens.etsmtl.ca; lyne.woodward@etsmtl.ca).

K. Al-Haddad is with the Canada Research Chair in Electrical Energy Conversion and Power Electronics, Montréal, QC H3C 1K3 Canada (e-mail: kamal.al-haddad@etsmtl.ca).

Color versions of one or more of the figures in this paper are available online at http://ieeexplore.ieee.org.

Digital Object Identifier 10.1109/TPEL.2017.2697821

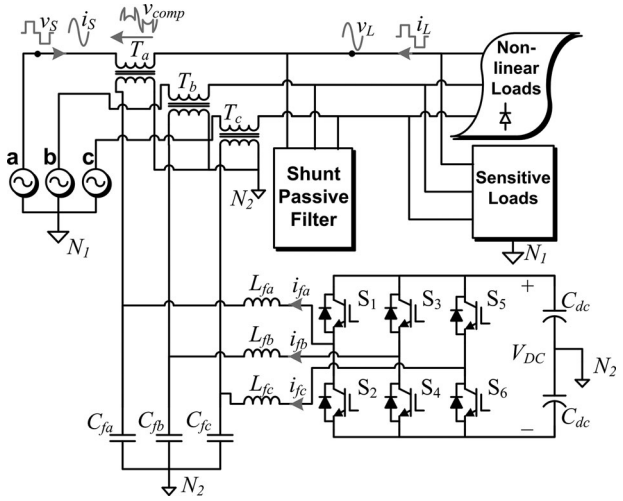

Fig. 2. Conventional hybrid SeAF topology.

TABLE I
SIMULATION AND EXPERIMENTAL PARAMETERS

Symbol	Definition	Value
V_S	Line-to-Line voltage	190–208 V_{rms}
f	System frequency	60 Hz
R_1^*, L_1^*	Linear Load #1	12.5 Ω, 40 mH
R^*, L^*	Nonlinear CSC load	12.5 Ω, 20 mH
Lf	Switching ripple filter inductance	5 mH
Cf	Switching ripple filter capacitance	0.5 μF
r_C	Switching ripple damping resistor	50 Ω
f_{PWM}	PWM frequency	8 kHz, 10 kHz*
V_{DC}	dc auxiliary power supply voltage	100–150 V
R	Non-linear load resistance	25 Ω
L	Non-linear load inductance	20 mH
S	Load power rating	2.6–3.1 kVA
K_P, K_r	Controller proportional and resonant gains	2.5, 10
ω_C	Cutoff frequency	5 rad/s
T_S	dSPACE, DS1103 Synchronous sampling time	42 μs

*Adopted value for the simulation analysis.

distortions and wrong computation of power and energy balance [19], [20]. This compensator could inject or absorb active power during grid voltage variations to ensure high-quality and reliable supply along with complete decoupling the grid from polluted loads.

II. Proposed System Architecture

A. System Configuration

Conventional series hybrid active filters have a common configuration as shown in Fig. 2 with a three-phase converter and three isolating transformers [21], [22], while the proposed configuration does not contain series transformers. The transformerless power hybrid filter shown in Fig. 3 is composed of a two-level H-bridge converter connected in series between the grid and the PCC, where the presented configuration allows an independent control on each individual phase regardless of the others. A bank of tuned passive filters ensures a low-impedance path for current harmonics. A dc bidirectional source is connected to inject power during voltage sags and absorbs it during overvoltage. In this paper, the studied system is implemented for a rated power of 8 kVA. For the rapid control prototyping (RCP) application and to ensure a fast transient response with sufficient stability margins over a wide range of dynamic operations, the controller is implemented on a dSPACE/dsp1103 real-time simulator. For an accurate real-time measurement of electrical variables, the Opal-RT OP8665 probes are performing the measurement task. System parameters are identified in Table I.

The studied loads consume 7.6 kW and exchange 2.3 kVAR with the network, resulting in a lagging power factor of 95 percent. A programmable source 120/208-V simulates several critical scenarios such as grid distortion, sag, or swell.

The THSeAF is connected in series in order to inject the compensating voltage. On the dc side of the compensator, auxiliary dc-link energy storage components are installed. The shunt passive filter constituted of several tuned filters is composed of a capacitor in series with an inductance with values tuned at desired frequency. Active filters are often keen to compensate current distortions, which is one of the priorities of the compensator. The current harmonics of the load produces voltage distortions when passing through the line and system impedances. Thus, to address such power quality issues, the proposed topology will be connected to the grid without the use of the bulky series transformer. This configuration will compensates source current harmonics and voltage distortion at the PCC.

B. Principle of the Hybrid Control Approach

The series active filter (SeAF) represents a controlled voltage-source inverter. In order to prevent current harmonics to drift into the power system, this series source should have a high-impedance characteristic for all harmonic components. The principle of such modeling is well documented in [23]. The use of a passive filter becomes mandatory to compensate current issues while maintaining a constant voltage free of harmonic distortions at the load terminals. The behavior of the SeAF for a current control approach is evaluated from the phasor's equivalent circuit shown in Fig. 4. The nonlinear load is modeled by a resistance representing the active power consumed and a current source generating harmonics current. Accordingly, the impedance Z_L represents the load. In this approach, the fundamental and harmonic components are analyzed together, not in two separate circuits.

The SeAF output voltage V_{Comp} is considered as an ideal controlled voltage source. If the control approach is based only on the detecting source current, the compensating voltage would be a gain (G) proportional to the current harmonics (I_{Sh}) flowing to the grid, the load voltage, as well as the source voltage harmonics. This approach gives results, which are less sensitive to the value of the gain G to achieve low level of current harmonic distortions

$$V_{\mathrm{Comp}} = +GI_{Sh} - V_{Lh} + V_{Sh}. \tag{1}$$

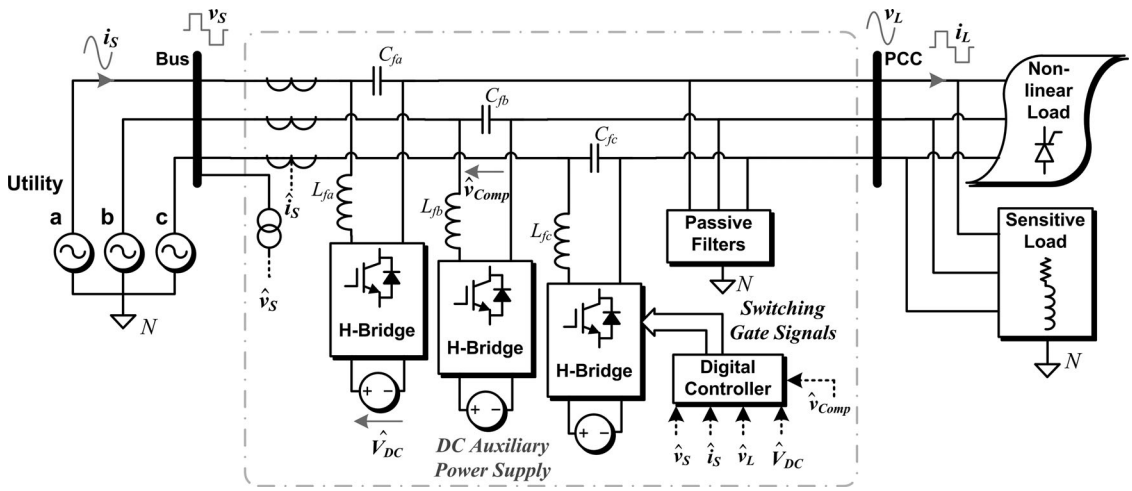

Fig. 3. Proposed three-phase THSeAF connected ahead of load PCC.

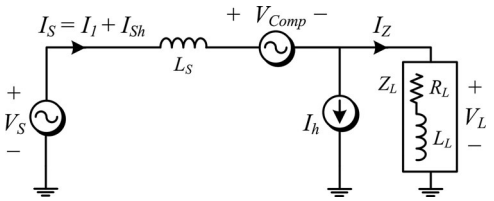

Fig. 4. Single-phase equivalent circuit for current harmonics.

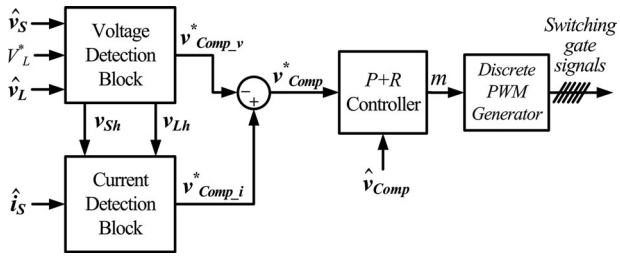

Fig. 5. Controller architecture scheme.

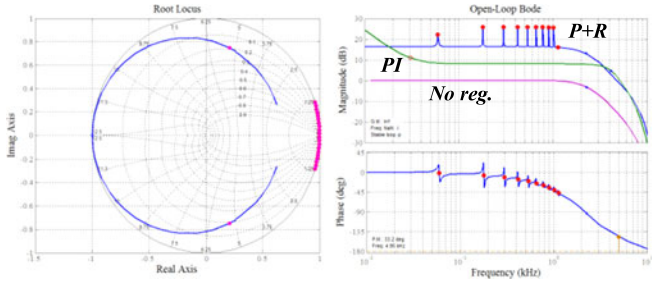

Fig. 6. Frequency response of the system including the 40-μs delay time. (a) Root locus diagram. (b) Bode diagram.

By substituting (1) into the system equations of Fig. 4, the two following variables are found:

$$I_{Sh} = \frac{(Z_L I_h + V_{Lh})}{(Z_S + Z_L + G)} \tag{2}$$

$$V_{Lh} = Z_L \ (I_{Sh} - I_h)\,. \tag{3}$$

By introducing (3) into (2), it became obvious that source current harmonics are completely eliminated independent of the value of the gain G

$$I_{Sh} = \frac{+Z_L I_h - Z_L I_h}{Z_S + Z_L + G} \ = \ 0. \tag{4}$$

Consequently, in this approach, even in the presence of source voltage distortions, the source current stays always clean of any harmonic component. An additional component is then added to regulate the load voltage terminals, which will be described in the next section. This extra component assists the THSeAF to operate similar to a DVR and maintain the load voltage regulated despite variation in the utility's voltage supply.

III. Control Algorithm of the THSeAF

A THSeAF configuration based on a VSC type of converter is considered in this section in order to avoid current harmonic pollution to flow into the grid [24]. The control strategy to compensate for current and voltage issues are based on the Park's transformation.

The inclusive diagram of the controller is illustrated in Fig. 5. The controller is mainly composed of three distinct parts: the voltage detection, current detection, and the P+R regulator [25]. The task attributed to each set of block is depicted in the present section.

Since in this paper the objective is to focus on the topology and the detection principle of the compensation, the regulator itself became less significant. Thus, a P+R regulator is implemented at this stage to demonstrate the effectiveness of the proposed configuration [26], [27]. The transfer function of the controller with a multiresonant property is given by

$$G_{\mathrm{P-R}}\ (s) = K_P \ + \sum_{h=1,3,5,7,\ldots}^{n} \frac{2K_{rh} \cdot \omega_C \cdot s}{s^2 + 2\omega_C \cdot s + (h \cdot \omega)^2} \tag{5}$$

where h is the harmonic order, K_p and K_{rh} are gains, $h\omega$ is the resonant frequency, and ω_C is the cutoff frequency. Their numerical values are depicted in Table I. The frequency responses with a delay time are depicted in Fig. 6, where the Bode

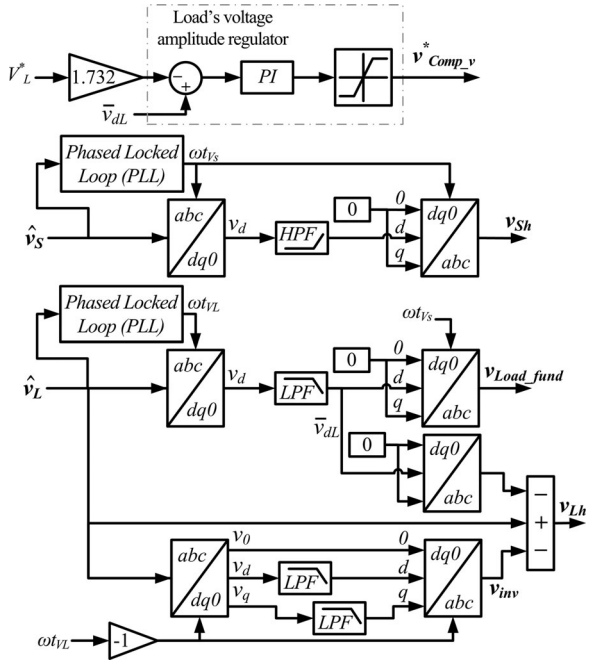

Fig. 7. Voltage detection control pattern.

diagram shows the superiority of the PR controller over the system without regulation and with a PI regulator.

z is the variable in the z-domain and T is the sampling time constant also known as step time T_S in MATLAB environment. The Bilinear approximation (Tustin) results in the following discrete transfer function in the z-domain as (6) shown at the bottom of this page.

According to the two developed discrete functions, one can implement either of them for a real-time simulation or a practical experiments on a digital controller.

The choice of gains is tied with the stability study of the transfer function. The gains should be chosen depending on the sampling time imposed by the digital controller and the behavior of the system itself, as shown in Fig. 6. In a general rule, the more the sampling time T_S has a smaller value, the more the chance to reach a stable system is observed. In the previous stage of the controller, as depicted in Fig. 5, after the voltage and currents are measured on a discrete sampling basis, the task to extract components, which should be eliminated, is underway.

Ahead of other block sets, the voltage detector using the synchronous reference frame (SRF) extracts first the fundamental component of load voltage, as depicted in Fig. 7. The *dq0* transformation is applied to produce each of the components, as illustrated in Fig. 7. To produces the $\boldsymbol{v}_{Sh}$, it is applied to the source voltage, where by extracting high-frequency oscillating portion of the direct component, the resultant source harmonics are obtained.

A reverse Park's transformation is required to obtain the three-phase compensation voltage. The three signals are summed with other compensating components and then sent to a pulse width modulator [28] to generate gate signals for the insulated-gate bipolar transistor converters

$$\boldsymbol{T} = \sqrt{\frac{2}{3}} \begin{bmatrix} \cos(\omega t) & \cos(\omega t - 2\pi/3) & \cos(\omega t + 2\pi/3) \\ \sin(\omega t) & \sin(\omega t - 2\pi/3) & \sin(\omega t + 2\pi/3) \\ 1/\sqrt{2} & 1/\sqrt{2} & 1/\sqrt{2} \end{bmatrix}$$

$$\boldsymbol{v}_{dq0} = \begin{bmatrix} v_d \\ v_q \\ v_0 \end{bmatrix} = \boldsymbol{T} \cdot \begin{bmatrix} v_a \\ v_b \\ v_c \end{bmatrix}. \tag{7}$$

To extract the load voltage harmonics during unbalance circumstances, the SRF is used to extract the inverse and zero-sequence component. By employing and inverted load's angular frequency and a tuned low-pass filter to extract the oscillating portions, it is made possible to obtain the $\boldsymbol{v}_{\text{inv}}$ in the *dq0* coordinate and then in the *abc* frame as follows:

$$\boldsymbol{v}_{\text{inv}}(dq0) = \begin{bmatrix} -\tilde{v}_d \\ -\tilde{v}_q \\ -v_0 \end{bmatrix} \tag{8}$$

$$\boldsymbol{v}_{\text{inv}}(abc) = \boldsymbol{T}^{-1}(-\omega t_{VL}) \times \boldsymbol{v}_{\text{inv}}(dq0). \tag{9}$$

To regulate and restore the load voltage, a term is added, which consisted of comparing the direct value of the load side to a constant reference. A P+R is then regulating this error during sag, swell, and unbalance. The auxiliary dc supplies the amount of power required to establish a regulated load voltage.

To compensate current distortions, the current detection block is operating, as illustrated in detail in Fig. 8. The *p-q theory* is used for the task of extracting the harmonics, unbalance, and other current-related issues. To do so, instantaneous voltage and current space vectors ***v*** and ***i*** in the $\alpha\beta 0$ coordinate are obtained using Clarke's transformation

$$\boldsymbol{C} = \sqrt{\frac{2}{3}} \begin{bmatrix} 1 & -1/2 & -1/2 \\ 0 & \sqrt{3}/2 & -\sqrt{3}/2 \\ 1/\sqrt{2} & 1/\sqrt{2} & 1/\sqrt{2} \end{bmatrix}$$

$$\boldsymbol{i}_{\alpha\beta 0} = \begin{bmatrix} i_\alpha \\ i_\beta \\ i_0 \end{bmatrix} = \boldsymbol{C} \times \begin{bmatrix} i_a \\ i_b \\ i_c \end{bmatrix}, \ \boldsymbol{v}_{\alpha\beta 0} = \begin{bmatrix} v_\alpha \\ v_\beta \\ v_0 \end{bmatrix} = \boldsymbol{C} \times \begin{bmatrix} v_{an} \\ v_{bn} \\ v_{cn} \end{bmatrix}. \tag{10}$$

$$G_{P+R}(z) = K_P + \sum_{h=1,3,5,7,\ldots}^{n} \frac{2K_{rh} \cdot \omega_C \cdot z^2 \cdot T - K_{rh} \cdot \omega_C \cdot T}{\left(1 + \omega_C T + (h\omega T)^2\right) z^2 + \left(\frac{(h\omega T)^2}{2} - 2\right) z + 1 - \omega_C T + \frac{(h\omega T)^2}{4}} \tag{6}$$

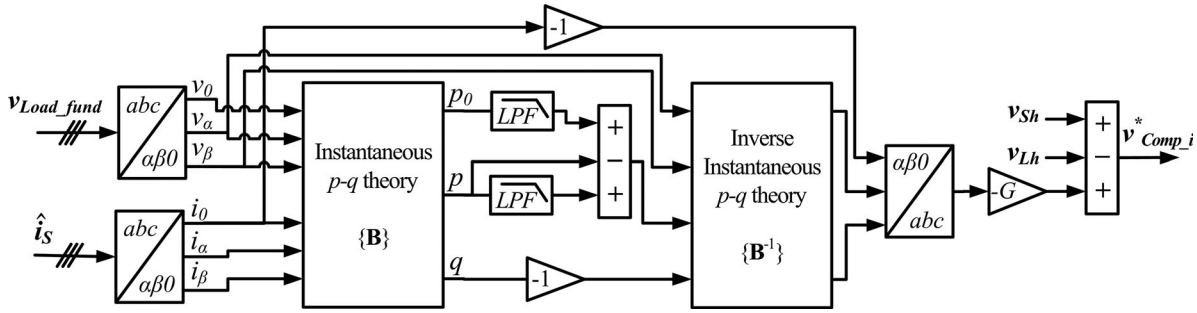

Fig. 8. Current issues detection diagram.

Thereafter, the instantaneous powers are defined

$$\begin{bmatrix} p \\ q \\ p_0 \end{bmatrix} = \underbrace{\begin{bmatrix} v_\alpha & v_\beta & 0 \\ v_\beta & -v_\alpha & 0 \\ 0 & 0 & v_0 \end{bmatrix}}_{\boldsymbol{B}} \begin{bmatrix} i_\alpha \\ i_\beta \\ i_0 \end{bmatrix}. \tag{11}$$

With reference to the $\alpha\beta 0$ coordinate, the powers are produced with the load's fundamental component but in phase with the source voltage. Obtained currents from the power expressions are decomposed into active and reactive parts. They were then used for current compensation purposes

$$\begin{bmatrix} i_\alpha \\ i_\beta \end{bmatrix} \triangleq \overbrace{\begin{bmatrix} i_{\alpha p} \\ i_{\beta p} \end{bmatrix}}^{i_p} + \overbrace{\begin{bmatrix} i_{\alpha q} \\ i_{\beta q} \end{bmatrix}}^{i_q} = \frac{1}{{v_\alpha}^2 + {v_\beta}^2} \begin{bmatrix} v_\alpha & v_\beta \\ v_\beta & -v_\alpha \end{bmatrix} \begin{bmatrix} p \\ 0 \end{bmatrix} + \frac{1}{{v_\alpha}^2 + {v_\beta}^2} \begin{bmatrix} v_\alpha & v_\beta \\ v_\beta & -v_\alpha \end{bmatrix} \begin{bmatrix} 0 \\ q \end{bmatrix} \tag{12}$$

where $(i_{\alpha p},\, i_{\beta p})$ are instantaneous active currents and $(i_{\alpha q},\, i_{\beta q})$ are instantaneous reactive currents. Both active and reactive powers can be divided into a constant amplitude component and an oscillating component: $p = \bar{p} + \tilde{p}$ and $q = \bar{q} + \tilde{q}$. By compensating the reactive portion of current, a conventional unity power factor ($\cos \emptyset \cong 1$) is obtained. Due to the presence of both zero-sequence currents and voltages in a four-wire system, p_0 must be considered for compensation. The oscillating portion of the active power and the zero-sequence power, if this latter exists, are compensated

$$\boldsymbol{B}^{-1} = \begin{bmatrix} \dfrac{v_\alpha}{{v_\alpha}^2 + {v_\beta}^2} & \dfrac{v_\beta}{{v_\alpha}^2 + {v_\beta}^2} & 0 \\ \dfrac{v_\beta}{{v_\alpha}^2 + {v_\beta}^2} & \dfrac{-v_\alpha}{{v_\alpha}^2 + {v_\beta}^2} & 0 \\ 0 & 0 & \dfrac{1}{v_0} \end{bmatrix} = \frac{1}{{v_0}^2 \left({v_\alpha}^2 + {v_\beta}^2\right)} \begin{bmatrix} {v_0}^2 v_\alpha & {v_0}^2 v_\beta & 0 \\ {v_0}^2 v_\beta & -{v_0}^2 v_\alpha & 0 \\ 0 & 0 & v_0 \left({v_\alpha}^2 + {v_\beta}^2\right) \end{bmatrix}. \tag{13}$$

Compensating instantaneous active and reactive currents are obtained as follows:

$$\boldsymbol{i}_p\,(\alpha\beta 0) = \boldsymbol{B}^{-1} \times \begin{bmatrix} -\tilde{p} \\ 0 \\ p_0 \end{bmatrix}, \quad \boldsymbol{i}_q\,(\alpha\beta 0) = \boldsymbol{B}^{-1} \times \begin{bmatrix} 0 \\ -q \\ 0 \end{bmatrix} \tag{14}$$

$$\boldsymbol{v}_{ih}\,(\text{abc}) = -G \times \left(\boldsymbol{C}^{-1} \times \begin{bmatrix} \boldsymbol{i}_p\,(\alpha\beta 0) \\ \boldsymbol{i}_q\,(\alpha\beta 0) \\ -\boldsymbol{i}_0 \end{bmatrix} \right) \tag{15}$$

where $\boldsymbol{C}^{-1}$ is the Clarke's reverse transform matrix. The three-phase voltage reference compensates the current harmonics produced by a nonlinear load. The interesting spot line to implement the current compensator is that it compensates the voltage harmonics as they generate current harmonics consequently. The current is then transformed to a relative three-phase voltage using a gain (G). In order that the THSeAF operates in optimal conditions, as defined in Section II-B, two extra terms are required to make compensation with low gain G under grid perturbations

$$\boldsymbol{v}^*_{\text{Comp\_}i}\ (abc) = -\left(G\boldsymbol{i}_{Sh} + \boldsymbol{v}_{Lh} - \boldsymbol{v}_{Sh}\right). \tag{16}$$

To conclude, the generic compensating voltage reference is reached by combination of the stated components related to current issues and voltage issues together

$$\boldsymbol{v}^*_{\text{comp}} = -\boldsymbol{v}_{\text{comp}_v} + \boldsymbol{v}_{\text{comp}_i}. \tag{17}$$

This reference is then compared with the measure output voltage of the compensator and by passing through the P+R regulator; the duty cycle $\boldsymbol{m}$ is produced. The duty cycle is a matrix of three components, each for a phase of the system.

IV. Simulation and Experimental Results

To analyze the behavior of the proposed topology to eradicate power quality issues, the system of Fig. 3 is implemented in MATLAB by applying a fixed discrete time T_S of 10 μs, which gives reliable results comparable to experimental implementation with parameters described in Table I.

In the simulation results shown in Fig. 9, the compensator starts operating at 0.05 s. It can be clearly observed that the major part of the source current harmonics is instantly

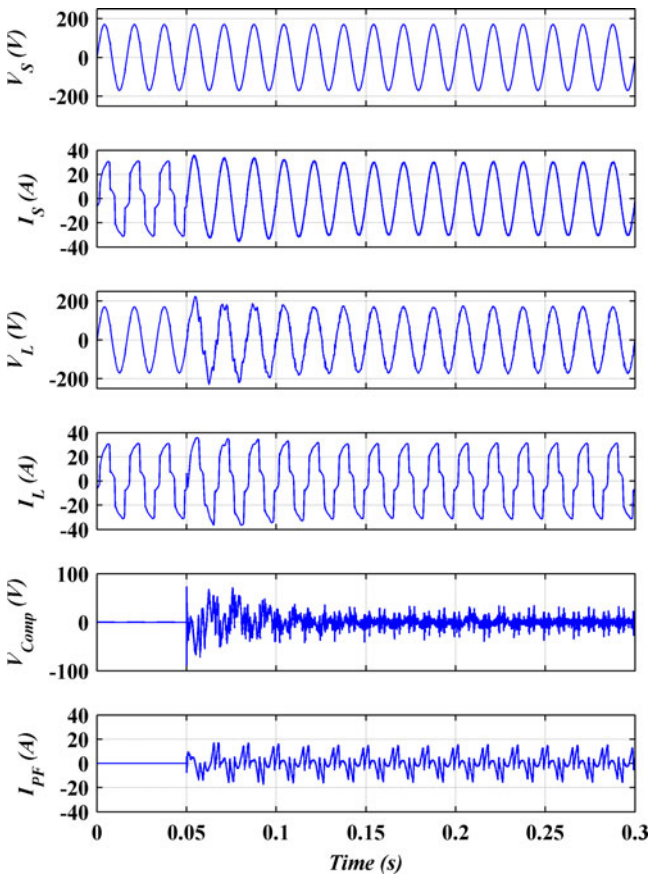

Fig. 9. Transformerless-HSeAF compensating current harmonics. (a) Source voltage v_S, (b) source current i_S, (c) load voltage v_L, (d) load current i_L, (e) active-filter voltage V_{Comp}, and (f) harmonics current of the HPF i_{HPF}.

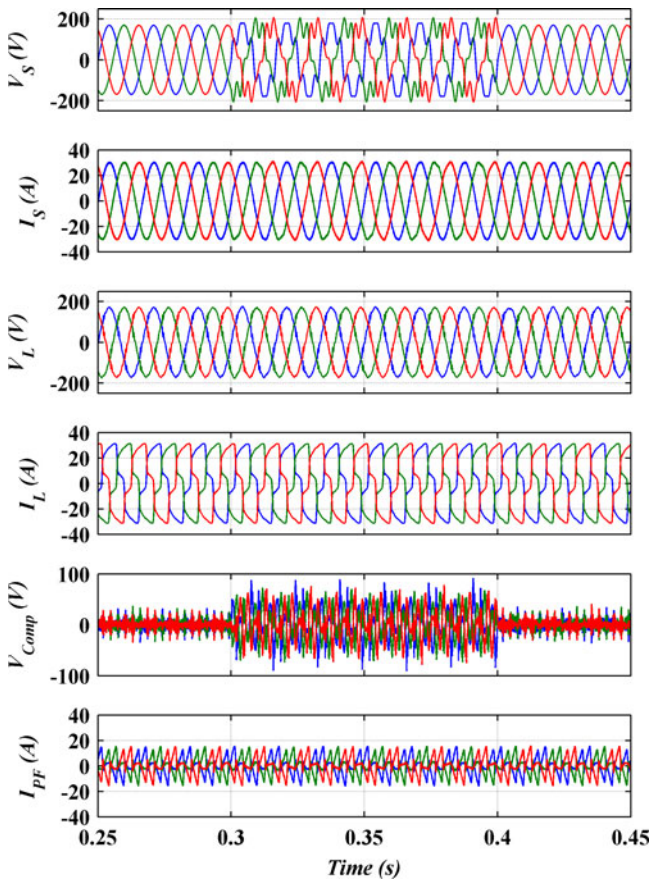

Fig. 10. Three-phase waveforms during grid's perturbation, while the THSeAF is enhancing the power quality.

compensated reaching a current's total harmonic distortion (THD) of 0.7%, whereas the load's current is highly polluted with a THD of 21%. The P+R regulator forces within three cycles the converter to follow the reference to produce the exact compensating voltage. The voltage generated by the compensator will force the nonlinear loads to draw a sinusoidal current in phase with the corresponding source voltage to achieve a unity power factor. The shunt passive filter in the configuration is essential to prevent current harmonics to flow into the grid. The compensator does not interfere with the active power flow; meanwhile, it has the ability to control the power flow by lagging or leading the current.

During voltage perturbations, the compensator maintains a harmonic-free and regulated voltage at the load terminals. –Fig. 10 demonstrates the behavior of the system during utility's voltage highly pollution with fifth- and seventh-order harmonics with 20% and 15% of the fundamental, respectively, resulting in a three-phase supply $(\boldsymbol{v}_S)$ containing a THD of 25%. The proposed compensator continues to clean the grid's current from harmonics and corrects the power factor, while the load's voltage THD is kept under the 5% limitation imposed by standards and regulations.

Fig. 11 illustrates the response of the system during source voltage unbalance (from 0.5 to 0.6 s and 0.7 to 0.8 s), while the filter regulates the load terminal voltage.

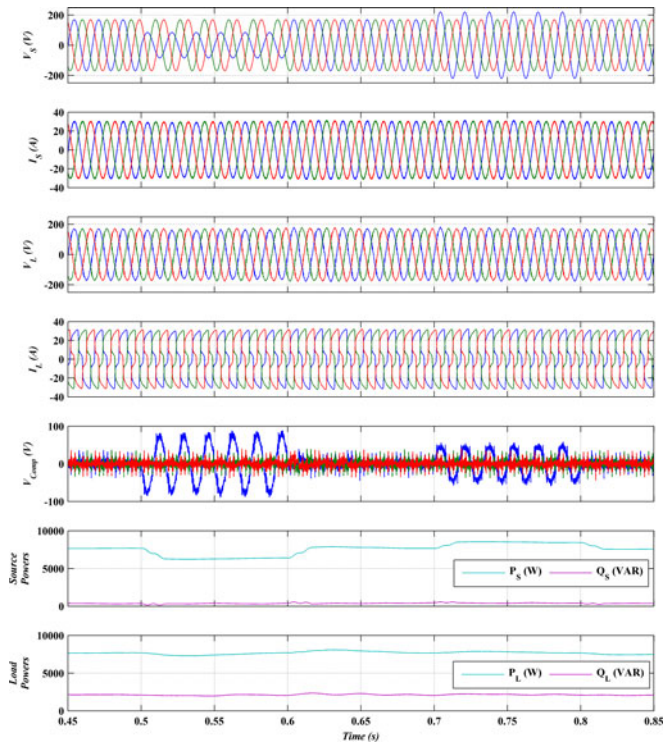

Fig. 11. Three-phase simulations during voltage unbalance with the THSeAF delivering a regulated and balanced supply to the load PCC.

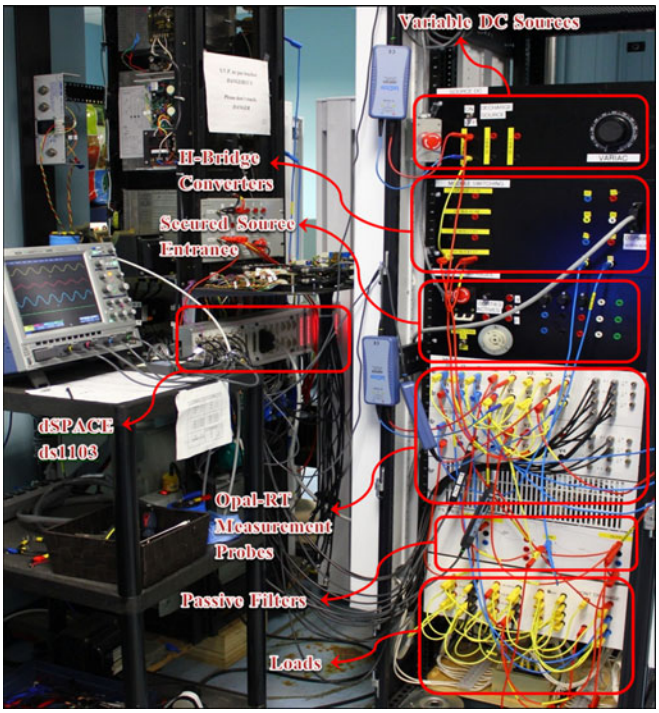

Fig. 12. Laboratory setup for the real-time THSeAF experimental tests.

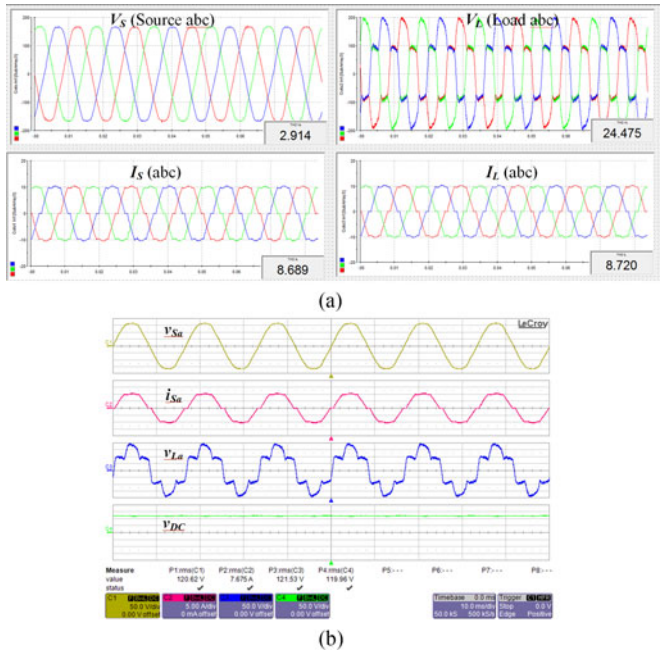

Fig. 13. TSeAF compensating load current harmonics. (a) 3φ dSPACE snapshot during operation of the real-time system. (b) Oscilloscope's measurement of one phase.

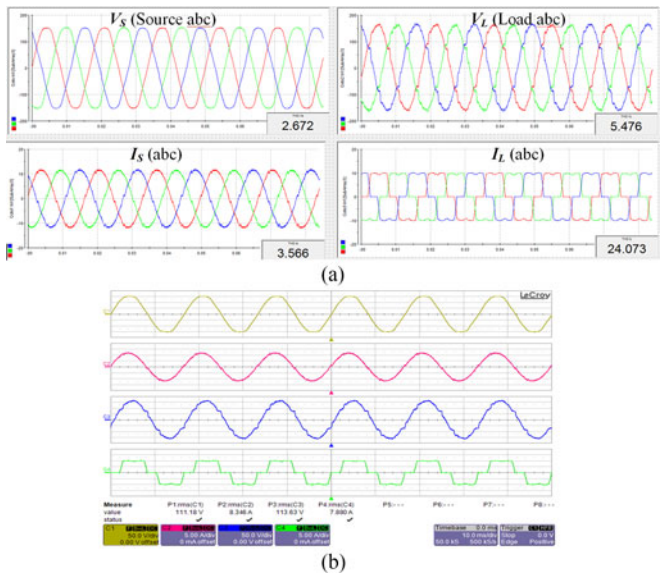

Fig. 14. THSeAF compensating load current harmonics. (a) dSPACE snapshot during operation of the real-time system. (b) Oscilloscope's measurement on phase A.

This active power compensator is able to follow variation in the load consumption while preventing current harmonics to flow into the grid side. Furthermore, it maintains a sinusoidal and regulated voltage across the PCC of loads.

The study is validated through the three-phase laboratory prototype realized according to the previous electric schema without the linear load. The RCP setup illustrated in Fig. 12 was realized to demonstrate efficiency and behavior of the proposed transformerless configuration.

The THSeAF is subjected to two kinds of compensation; within the first test, the compensator acting as an active filter cleans the source current, while during the second series of test, the compensator operates in a hybrid approach as explained in previous sections, regulating also the load's voltage in addition to the current harmonic compensation.

A. Load Current Harmonics Compensation

1) Transformerless Series Active Filter (TSeAF) Operation Without the Shunt Passive Filter Branch: In this section, only the active part is connected to operate as harmonic isolator and the shunt passive filter is not yet connected. In this test, the nonlinear load is connected solely to the PCC to have a higher degree of pollution. The TSeAF active's part is generating a voltage to force the load to draw a sinusoidal waveform current. To point out the importance of the compensation strategy developed in the previous section, the following tests are prepared with the nonlinear load (THD$i = 26.7\%$) connected to the PCC.

As endorsed previously, by including the voltage harmonics into the control law, better results are achieved. Fig. 13 demonstrates the results when $v_{\mathrm{Comp}} = +Gi_{Sh} - v_{Lh} + v_{Sh}$. The fact to have these components implicated in the control process allows reducing considerably the harmonic gain G and obtaining fairly enhanced results. With intact output converter's filter, the harmonic distortion is reduced to 8.6%, with a small gain G of 3.7.

2) THSeAF Operating With a Shunt Passive Filter: In the following tests, the shunt passive filter branch is connected to help improving the load's voltage and creating a low-impedance pathway for current harmonics coming from the load.

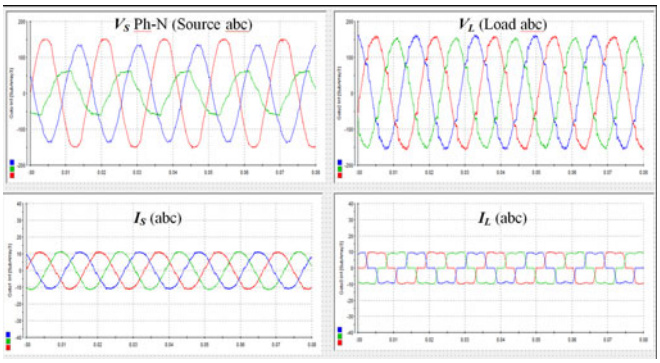

Fig. 15. dSPACE snapshot during a real-time operation of the THSeAF compensating current harmonics and performing voltage restoration.

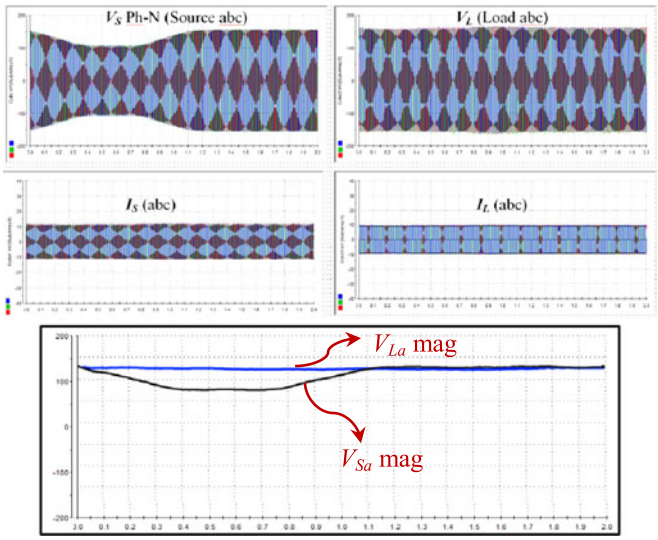

Fig. 16. Three-phase THSeAF compensating in real time the load current harmonics and performing voltage regulation during sags.

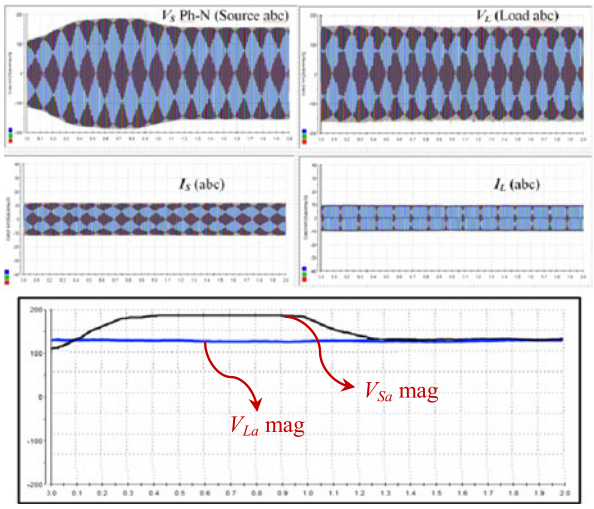

Fig. 17. Three-phase THSeAF compensating in real time the load current harmonics and performing voltage regulation during Swells.

The nominal voltage is reduced to 110-Vrms ph-N, and consequently, the rating of the system is reduced to 2.6 kVA. With the passive filter, the active part performs more reliable as it requires lower compensating voltage and less stiffness to achieve desired result. Related waveforms captured from the experimental prototype are summarized in Fig. 14. The results are obtained at reduced dc voltage 100 Vdc.

After compensation, the THSeAF forces the current harmonics to circulate into the shunt passive filter and cleans the source current from undesired harmonics. The following table illustrates clearly that the current flowing into the grid is now ridded of harmonics, and the THD of i_S achieves 3.5%.

B. THSeAF in Hybrid Compensation of Both Current and Voltage Issues

The THSeAF is aimed to compensate bulk issues related to voltage and current simultaneously. To achieve this objective, the controller developed earlier is implemented to regulate the load voltage in addition to source current compensation. The compensator will operate similar to a DVR to restore the load voltage despite perturbation in the grid's supply. In these experiments, two tests are performed: the supply voltage unbalance and the sags and swells. In both essays, it is noticed that the load voltage remains regulated.

Fig. 15 demonstrates experimental results for the three-phase system. The compensator is compensating and performing a restoration of a balanced three-phase voltage while compensating load current simultaneously. The auxiliary dc supply for each phase is maintained at 110 Vdc. The load voltage is regulated at the nominal value of 110 Vrms Ph-N.

The series hybrid active filter is advantageous when the grid voltage is subjected to sags and swells, as shown in Figs. 16 and 17. Under such circumstances, the three-phase source (grid) voltage amplitude is reduced during multiple cycles. The compensator will absorb or inject required amount of active power to maintain the load voltage amplitude at a constant value.

V. Conclusion

With the ever increase of renewable sources connected to the smart grid via various resonant filters interacting with the grid impedances and causing undesired EMI phenomenon, it became essential to maintain a clean and decoupled power distribution system. In this paper, a three-phase THSeAF based on VSC type of converters was introduced to improve power quality issues of the distribution level of the grid. The proposed control algorithm consisting of the SRF and the *p-q theory* was developed to extract voltage and current harmonics as well as unbalance, sags, and swells to be compensates. The key novelty of the proposed topology includes power quality improvement for small residential building and some low-voltage distribution system that may result to the enhancement of the global power system.

Furthermore, the proposed configuration can regulate and improve the load voltage PCC, and when connected to a renewable auxiliary dc source, the topology is able to counteract actively to the power flow in the system similar to a UPS function. It was denoted that the active compensator responds seamlessly

to voltage variations by ensuring a constant and distortion-free supply at load PCC. Furthermore, this compensator eliminates source current harmonics and improves grid power quality with no need to use the typical bulky series transformer. By means of real-time RCP application, it was demonstrated that this active compensator responds properly to source voltage variations by providing a constant and distortion-free supply at load terminals. Furthermore, the results showed that by eliminating source harmonic currents and unbalances, the global grid power quality will be assessed without the usual bulky and costly series transformer. The proposed transformerless active power filter was simulated and experimentally validated.

REFERENCES

[1] A. Javadi, A. Hamadi, A. Ndtoungou, and K. Al-Haddad, "Power quality enhancement of smart households using a multilevel-THSeAF with a PR controller," *IEEE Trans. Smart Grid*, vol. 8, no. 1, pp. 465–474, Jan. 2017.

[2] S. Rivera, W. Bin, S. Kouro, V. Yaramasu, and W. Jiacheng, "Electric vehicle charging station using a neutral point clamped converter with bipolar DC bus," *IEEE Trans. Ind. Electron.*, vol. 62, no. 4, pp. 1999–2009, Apr. 2015.

[3] A. F. Zobaa, "Optimal multiobjective design of hybrid active power filters considering a distorted environment," *IEEE Trans. Ind. Electron.*, vol. 61, no. 1, pp. 107–114, Jan. 2014.

[4] L. Hernandez *et al.*, "A survey on electric power demand forecasting: future trends in smart grids, microgrids and smart buildings," *IEEE Commun. Surveys Tuts.*, vol. 16, no. 3, pp. 1460–1495, Third Quarter 2014.

[5] G. Qinglai, X. Shujun, S. Hongbin, L. Zhengshuo, and Z. Boming, "Rapid-charging navigation of electric vehicles based on real-time power systems and traffic data," *IEEE Trans. Smart Grid*, vol. 5, no. 4, pp. 1969–1979, Jul. 2014.

[6] A. Javadi and K. Al-Haddad, "A single-phase active device for power quality improvement of electrified transportation," *IEEE Trans. Ind. Electron.*, vol. 62, no. 5, pp. 3033–3041, May 2015.

[7] T. Quoc-Nam and L. Hong-Hee, "Improvement of unified power quality conditioner performance with enhanced resonant control strategy," *IET Gener., Transmiss. Distrib.*, vol. 8, pp. 2114–2123, 2014.

[8] A. Q. Ansari, B. Singh, and M. Hasan, "Algorithm for power angle control to improve power quality in distribution system using unified power quality conditioner," *IET Gener., Transmiss. Distrib.*, vol. 9, pp. 1439–1447, 2015.

[9] W. Yanzhi, L. Xue, and M. Pedram, "Adaptive control for energy storage systems in households with photovoltaic modules," *IEEE Trans. Smart Grid*, vol. 5, no. 2, pp. 992–1001, Mar. 2014.

[10] E. C. D. Santos, J. H. G. Muniz, E. R. Cabral da Silva, and C. B. Jacobina, "Nested multilevel topologies," *IEEE Trans. Power Electron.*, vol. 30, no. 8, pp. 4058–4068, Aug. 2015.

[11] S. Kouro, J. I. Leon, D. Vinnikov, and L. G. Franquelo, "Grid-connected photovoltaic systems: An overview of recent research and emerging PV converter technology," *IEEE Ind. Electron. Mag.*, vol. 9, no. 1, pp. 47–61, Mar. 2015.

[12] M. S. Hamad, M. I. Masoud, and B. W. Williams, "Medium-voltage 12-pulse converter: Output voltage harmonic compensation using a series APF," *IEEE Trans. Ind. Electron.*, vol. 61, no. 1, pp. 43–52, Jan. 2014.

[13] J. Liu, S. Dai, Q. Chen, and K. Tao, "Modelling and industrial application of series hybrid active power filter," *IET Power Electron*., vol. 6, pp. 1707–1714, 2013.

[14] A. Javadi, A. Hamadi, L. Woodward, and K. Al-Haddad, "Experimental investigation on a hybrid series active power compensator to improve power quality of typical households," *IEEE Trans. Ind. Electron.*, vol. 63, no. 8, pp. 4849–4859, Aug. 2016.

[15] Y. Lu, G. Xiao, X. Wang, F. Blaabjerg, and D. Lu, "Control strategy for single-phase transformerless three-leg unified power quality conditioner based on space vector modulation," *IEEE Trans. Power Electron.*, vol. 31, no. 4, pp. 2840–2849, Apr. 2016.

[16] B. W. Franca, L. F. da Silva, M. A. Aredes, and M. Aredes, "An improved iUPQC controller to provide additional grid-voltage regulation as a STATCOM," *IEEE Trans. Ind. Electron.*, vol. 62, no. 3, pp. 1345–1352, Mar. 2015.

[17] A. Javadi, A. Ndtoungou, H. F. Blanchette, and K. Al-Haddad, "Power quality device for future household systems with fast electric vehicle charging station," in *Proc. IEEE Veh. Power Propulsion Conf.*, Montreal, QC, Canada, 2015, pp. 1–6.

[18] A. Javadi, A. Hamadi, and K. Al-Haddad, "Three-phase power quality device for weak systems based on SRF and p-q theory controller," in *Proc. 41st Annu. Conf. IEEE Ind. Electron. Soc.*, Yokohama, Japan, 2015, pp. 345–350.

[19] K. Rahbar, X. Jie, and Z. Rui, "Real-time energy storage management for renewable integration in microgrid: An off-line optimization approach," *IEEE Trans. Smart Grid*, vol. 6, no. 1, pp. 124–134, Jan. 2015.

[20] A. Javadi, G. Olivier, and F. Sirois, "A real-time power hardware-in-the-loop implementation of an active filter," *Przegląd Elektrotechniczny (Electr. Rev.)*, vol. 86/11a, pp. 7–13, Nov. 2010.

[21] S. Bhattacharya, C. Po-Tai, and D. M. Divan, "Hybrid solutions for improving passive filter performance in high power applications," *IEEE Trans. Ind. Appl.*, vol. 33, no. 3, pp. 732–747, May/Jun. 1997.

[22] C. Po-Tai, S. Bhattacharya, and D. Divan, "Experimental verification of dominant harmonic active filter for high-power applications," *IEEE Trans. Ind. Appl.*, vol. 36, no. 2, pp. 567–577, Mar./Apr. 2000.

[23] H. Fujita and H. Akagi, "A practical approach to harmonic compensation in power systems-series connection of passive and active filters," *IEEE Trans. Ind. Appl.*, vol. 27, no. 6, pp. 1020–1025, Nov./Dec. 1991.

[24] J. H. Kim, S. K. Sul, and P. N. Enjeti, "A carrier-based PWM method with optimal switching sequence for a multilevel four-leg voltage-source inverter," *IEEE Trans. Ind. Appl.*, vol. 44, no. 4, pp. 1239–1248, Jul./Aug. 2008.

[25] L. Y. Wei, F. Blaabjerg, D. M. Vilathgamuwa, and L. P. Chiang, "Design and comparison of high performance stationary-frame controllers for DVR implementation," *IEEE Trans. Power Electron.*, vol. 22, no. 2, pp. 602–612, Mar. 2007.

[26] W. Rong-Jong, L. Chih-Ying, H. Yu-Chih, and C. Yung-Ruei, "Design of high-performance stand-alone and grid-connected inverter for distributed generation applications," *IEEE Trans. Ind. Electron.*, vol. 60, no. 4, pp. 1542–1555, Apr. 2013.

[27] D. Ricchiuto, M. Liserre, T. Kerekes, R. Teodorescu, and F. Blaabjerg, "Robustness analysis of active damping methods for an inverter connected to the grid with an LCL-filter," in *Proc. Energy Convers. Congr. Expo.*, 2011, pp. 2028–2035.

[28] P. N. Enjeti, P. D. Ziogas, J. F. Lindsay, and M. H. Rashid, "A new PWM speed control system for high-performance AC motor drives," *IEEE Trans. Ind. Electron.*, vol. 37, no. 2, pp. 143–151, Apr. 1990.

Alireza Javadi (S'09–M'16) received the B.Sc. degree in power electrical engineering from K.N. Toosi University of Technology, Tehran, Iran, and the M.Sc.A. degree in electrical engineering from the École Polytechnique de Montréal, Montreal, QC, Canada, in 2007 and 2009, respectively, and the Ph.D. degree in electrical engineering from the École de Technologie Supérieure (ÉTS), Montreal, in 2016.

He is currently a Postdoctoral Fellow with the NSERC-CRSNG, the Canada Research Chair in Electrical Energy Conversion and Power Electronics, ETS. His research interests encompass power electronics converters, harmonics and reactive power control using hybrid active filters, power quality of Smart grids, renewable energy, fast electric vehicle charging stations, real-time power hardware-in-the-loop applications, and rapid control prototyping.

Dr. Javadi was an active member of the IEEE Montreal section and a former president of the IEEE-ÉTS.

Lyne Woodward (M'11) received the B.Sc. degree in electrical engineering from the University of Sherbrooke, Sherbrooke, QC, Canada, in 1994, and the M.Sc.A. and Ph.D. degrees in chemical engineering from the Ecole Polytechnique de Montréal, Montréal, QC, in 2003 and 2009, respectively.

From 1995 to 2004, she was an Engineer in the Process Control Department of Hatch. Since 2010, she has been an Associate Professor with the Department of Electrical Engineering, École de Technologie Supérieure, Montréal. She is also the Director of the Groupe de Recherche en Commande Industrielle et Électronique de Puissance that includes more than 100 members. Her research interests include real-time optimization, control of linear and nonlinear systems, optimal conversion and management of renewable energy such as wind energy, solar energy, and bioenergy.

Kamal Al-Haddad (S'82−M'88−SM'92−F'07) received the B.Sc.A. and M.Sc.A. degrees in electrical engineering from the University of Québec à Trois-Rivières, Trois-Rivières, Canada, in 1982 and 1984, respectively, and the Ph.D. degree in electrical engineering from the Institute National Polythechnique, Toulouse, France, in 1988.

Since June 1990, he has been a Professor with the Department of Electrical Engineering, École de Technologie Supérieure, Montréal, QC, Canada, where he has been the holder of the Senior Canada Research Chair in Electric Energy Conversion and Power Electronics since 2002. He has supervised more than 100 Ph.D. and M.Sc.A. students working in the field of power electronics. He is a Consultant and has established very solid link with many Canadian industries working in the field of power electronics, electric transportation, aeronautics, and telecommunications. He has coauthored more than 500 IEEE transactions and conference papers. His fields of interest are in high-efficient static power converters, harmonics and reactive power control using hybrid filters, switch-mode and resonant converters including the modeling, control, and development of prototypes for various industrial applications in electric traction, renewable energy, power supplies for drives, telecommunication, etc.

Prof. Al-Haddad is a Fellow of the Canadian Academy of Engineering. He is the President of the IEEE Industrial Electronics Society (IES) for 2016–2017, an Associate editor of the IEEE TRANSACTIONS ON INDUSTRIAL INFORMATICS, and an IES Distinguished Lecturer. He has received the Dr.-Ing. Eugene Mittelmann Achievement Award.